CIRCULATION AND SALINITY DISTRIBUTION IN A MARSH-LAKE SYSTEM IN COASTAL LOUISIANA

By

Björn Kjerfve

CENTER for WETLAND RESOURCES

LOUISIANA STATE UNIVERSITY · BATON ROUGE

SG-72-06

CIRCULATION AND SALINITY DISTRIBUTION IN A MARSH-LAKE SYSTEM IN COASTAL LOUISIANA

by

Björn Kjerfve

Publication No. LSU-SG-72-06

Center for Wetland Resources
Louisiana State University
Baton Rouge, Louisiana

November 1972

This work is a result of research sponsored by NOAA Office of Sea Grant, Department of Commerce, under Grant #2-35231. The U.S. Government is authorized to produce and distribute reprints for governmental purposes notwithstanding any copyright notation that may appear hereon.

ABSTRACT

Repeated measurements of current velocity, conductivity, and temperature at 26 stations during an eight-day period in June 1971, plus tide and wind records from one location, provided insight into the physical oceanography of the Airplane Lake, Lake Palourde, and Lake Laurier section of coastal Louisiana west of the Mississippi River delta. Sampling was performed over the diurnal tide cycle with compensation for the fortnightly tidal period. An approximate method was devised to calculate the time-averaged discharge at each station, and it was found that the study area experienced a considerable net water loss during the period. This was accounted for by the "net wind stress." Time- and depth-averaged isohalines provided qualitative information about the fresh water supply to the area, and the low run-off limit was determined. However, it was not possible to assess the exact fresh water discharge without prior knowledge of the effective horizontal eddy diffusivity. The 50% renewal time of the water in the tri-lake system was calculated to be 12 diurnal cycles, assuming steady state conditions.

CONTENTS

FIGURES

TABLES

ACKNOWLEDGEMENTS

This investigation was sponsored by Louisiana State University's Office of Sea Grant Development. LSU's Sea Grant Program is part of the National Sea Grant Program, which is maintained by the National Oceanic and Atmospheric Administration of the U. S. Department of Commerce. Special thanks go to Dr. W. G. Smith, Mrs. A. Siripong, and Messrs. E. M. Bishop, C. D. Walters, and A. A. Pusch, who assisted in collecting the data.

INTRODUCTION

Louisiana State University has conducted Sea Grant funded marine-related research since 1968. The interdisciplinary program has concentrated on the Barataria-Caminada Bay region of coastal Louisiana with particular focus on a small area surrounding Airplane Lake on the western edge of Caminada Bay.

The physical oceanography has, until now, received only limited attention in comparison to biological, ecological, geological, and geochemical work. The aim of the present study is to describe the net circulation, salinity distribution, and flow characteristics of the complex marsh-water system in the vicinity of Airplane Lake, including Lake Palourde and Lake Laurier. Besides aiding in a better understanding of aspects of the physical oceanography, it is hoped that the information contained in this report will prove useful to the entire Sea Grant Systems Ecology project. Also, it is believed that the data may provide some of the needed boundary conditions for the transport models derived for this area (Hacker et al., 1970, 1971).

All reported field measurements were taken during an eight-day period, June 21-28, 1971. The study should therefore be considered as a pilot experiment, setting guidelines for future work. Care should be observed when extrapolating the presented results to other seasons and years.

SAMPLING DESIGN

Current speed and direction, conductivity, and temperature were measured at 26 locations throughout the study area (Fig. 1). In order to simplify the analysis, the readings were taken in the middle of bayous or restricted passages, where simple channel geometry indicated lack of secondary flows.

Marmer (1947) described the Barataria Bay tide, which is of the diurnal kind. Although the predominant tidal period barely exceeds 24 hours, Marmer pointed out the existence of longer term fluctuations. There is a fortnightly cycle due to the moon's declination. Also, there is an annual cycle, as well as a cycle of 18.67 years due to the longitude of the moon's node. The present study takes the diurnal and fortnightly cycles into consideration.

Sampling began three days after the occurrence of a tropical tide and ended three days prior to the following equatorial tide so that the results reflect average conditions over the fortnightly cycle for this time of year.

The sampling over the diurnal cycle was performed in a manner analogous to a two-way classification of variance, blocking on time. Each tidal cycle, as measured at station 13, was sub-divided into six stages (Fig. 2). Each station was visited at least once during each stage without respect to the particular tidal cycle chosen. Corrections had to be made for the unequal duration of falling and rising tides. Sample runs were based on the predicted tide at Caminada Pass, which did not exactly coincide with the actual tide stage measured at station

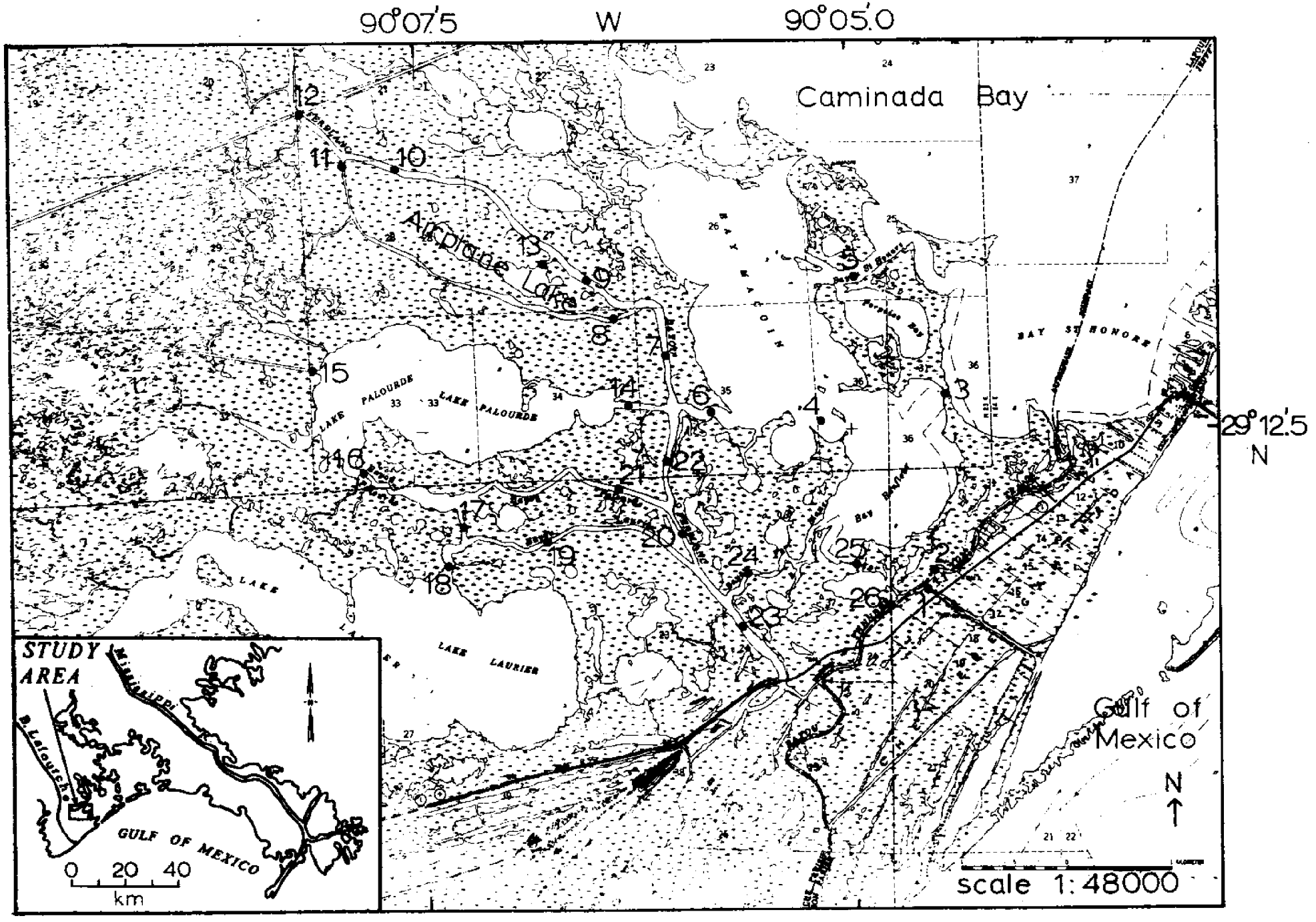

Figure 1. Map of study area showing the 26 sampling locations.

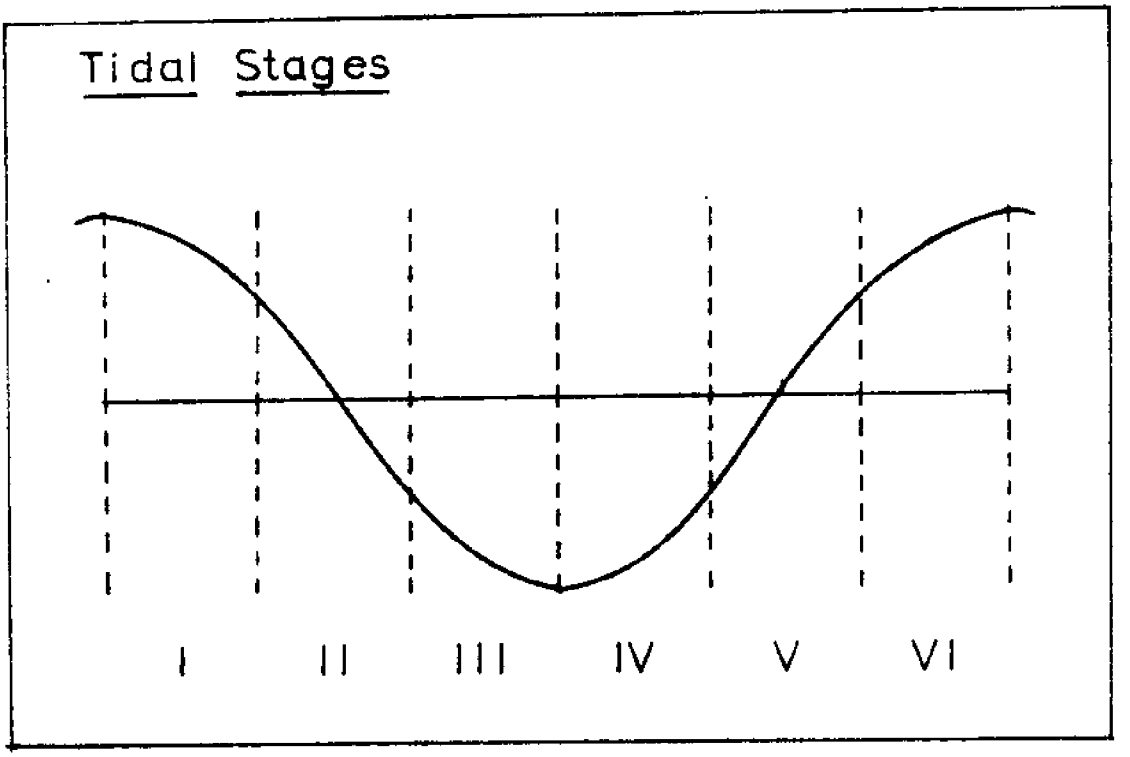

Figure 2. The tidal cycle, as measured at station 13, was subdivided into six stages. The figure shows an idealized tidal curve and the chosen duration of the stages.

13 and occasionally produced data gaps.

Along with the previously mentioned measurements, wind speed and direction and water level were automatically recorded at the permanent instrument station at the entrance to Airplane Lake (#13). The instrumentation maintained there was described by Adams (1970).

Mid-channel water depths were measured each time a station was occupied. Also, cross-sectional channel profiles were surveyed at seven representative stations (Fig. 3).

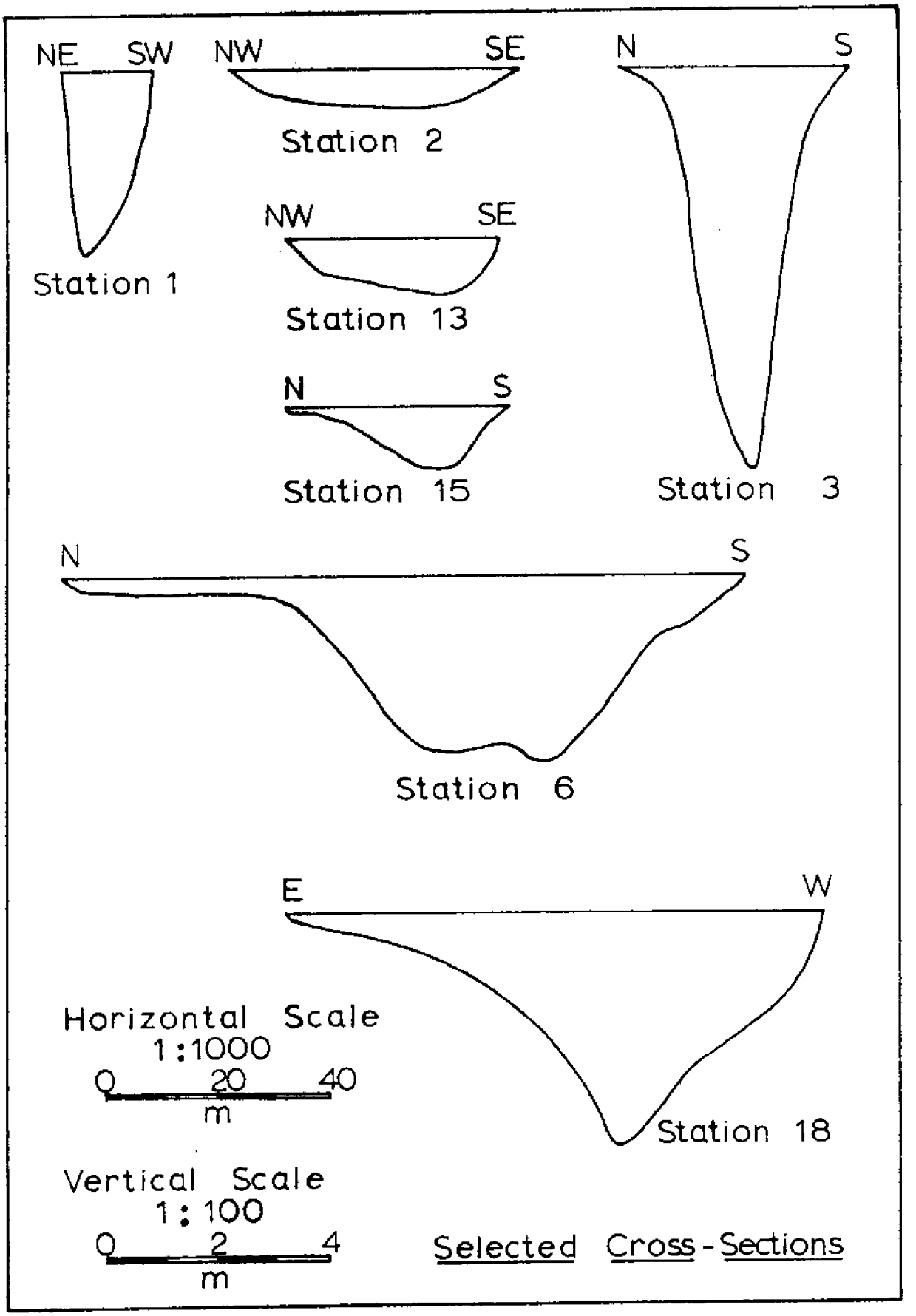

Figure 3. Seven representative cross-sections referred to the mean water level of the study period.

THE DATA

A. Tide Measurements

The water level was recorded automatically at station 13 every 15 minutes, using a Fischer-Porter digital water level recorder series 1542. The tide record is plotted in Figure 4. Indications are that the average water level (=13.48 ft) was unusually low for this time of year; however, data from previous years has not yet been reduced to allow a comparison.

Mean high water occurred 18.5 cm above the average height and mean low water 17.7 cm below, indicating a mean range of 36.2 cm. The fortnightly tide period is revealed by the gradual change in tidal range from a maximum of 46.0 cm on June 22, to a low of 23.2 cm on June 28.

The average diurnal tide period lasted 24.25 hours. The duration of the fall and rise was on the average 12.33 and 11.92 hours respectively. The record also reveals a slow shift in the tidal periodicity from 25.75 to 23.50 hours over the study period.

On the average, the high tide at Airplane Lake occurred 33 minutes after the predicted high tide for Caminada Pass, while the low tide was delayed by 104 minutes. The actual tide range at Airplane Lake was somewhat smaller than the predicted range for Caminada Pass.

B. Velocity Measurements

The current directions changed over the tidal cycle, and large fluctuations in magnitude were noticed. However, the measured velocity

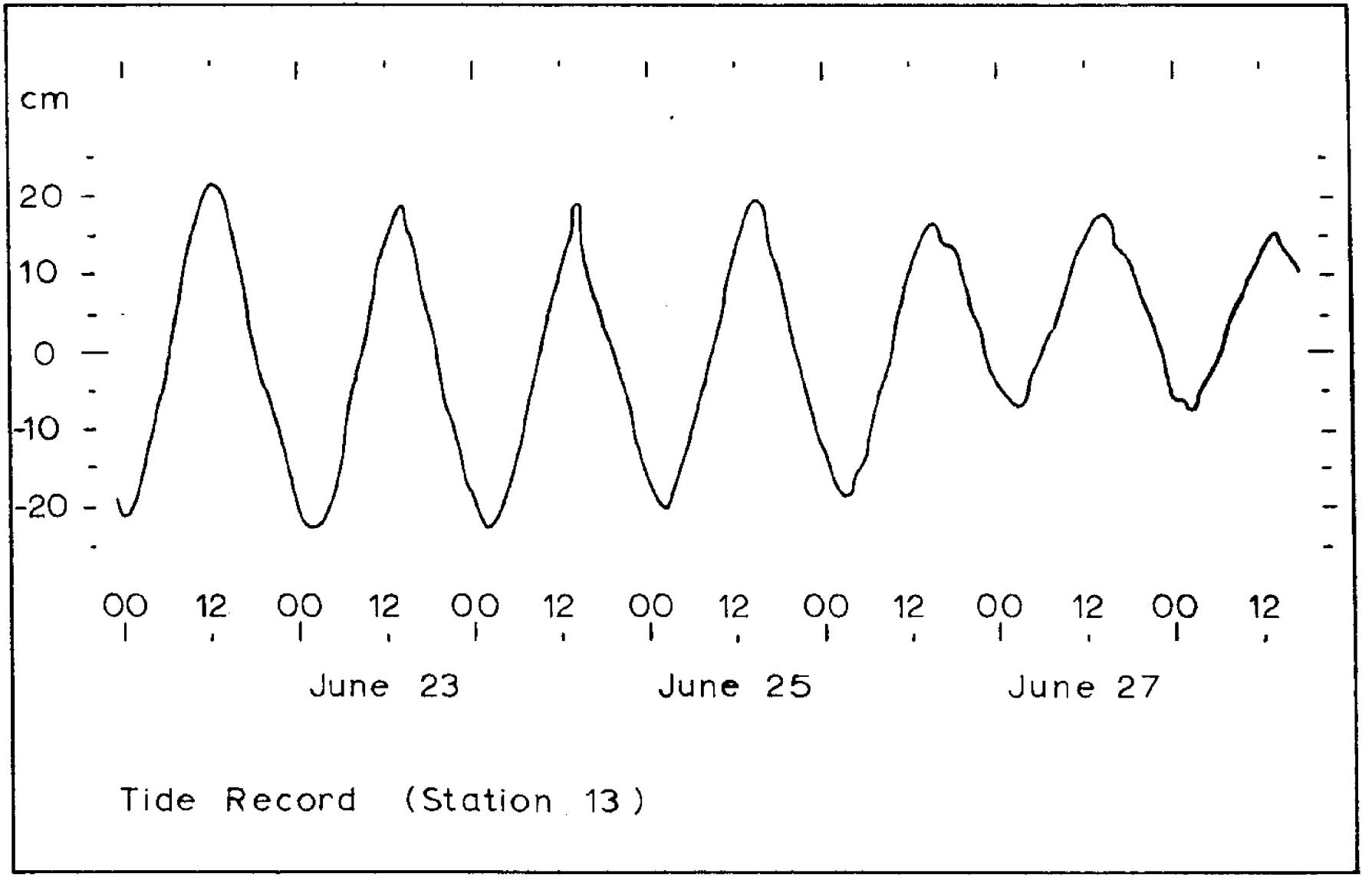

Figure 4. Measured tide record at station 13, referred to CDT.

vectors were for all practical purposes parallel to the banks at each station (except at #4) at all times.

Biplane current crosses (Pritchard and Burt, 1951) were used to measure all velocities. The angle, α, between the line attached to the submerged drag and the vertical was determined with an inclinometer. By knowing the drag's cross-sectional area, A, and the submerged mass, M, of the crosses, the velocity, v, was calculated from

$$v = [2Mg \tan(\alpha) / A\rho C_D]^{1/2} \qquad (1)$$

as derived by Pritchard and Burt, where g is the gravitational acceleration, ρ is the water density, and C_D is a non-dimensional drag coefficient.

The drag coefficient is a function of the object's shape and the Reynolds number. Rouse (1961) showed that for rectangular plates with a width-to-depth ratio of 1 to 5, C_D takes on a constant value of approximately 1.2 for all Reynolds numbers greater than 10^3. Let

$$\text{Re } \# = vD / \nu \quad > 10^3 \qquad (2)$$

where ν is the molecular viscosity ($\simeq 0.8 \times 10^{-2}$ cm^2 s^{-1} for a water temperature of 30°C), and D is the smallest side of any cross used (in this case D = 12 cm). It follows that equation 1 is theoretically sound for all velocities greater than 0.7 cm s^{-1}.

Also, Foerster (1968) statistically compared a small biplane current cross to two standard current meters: a Gurley 401 and a Gurley

Pigmy. He concluded that the agreement between cross and meters was highly significant (failed to reject the null hypothesis at the .99 level), and that the cross "was less devious in measuring current velocities" than the Gurley meters. Foerster's cited value of C_D = 1.2 was used in this study.

Two sets of three biplane crosses built out of 0.125 inch polyvinyl-chloride sheets were used in the present research. Each cross could be combined with either one of three weights. Pertinent information about the current crosses is presented in Table 1.

The crosses and weights were used in a combination such that the measured angle, α, varied between 0° and 40°. The angle could be determined to the nearest degree. The error is considered to be less than 2 cm s^{-1} and usually less than 1 cm s^{-1}, provided that the crosses were chosen correctly, i.e., large cross and light weight for slow currents and small cross and heavy weight for swift currents.

The velocities were measured in the middle of each channel in meter intervals from the surface to the bottom. A depth-correction factor of cos (α) was applied. The data is tabulated in the appendix. Each velocity reading was averaged by eye over 15 seconds to remove the highest frequency fluctuations. Also, due to the size of the crosses, each reading is not a point estimate but rather a velocity average over the area occupied by the cross. At extremely shallow stations, the current cross in fact measures a quantity approximately equal to the depth-averaged velocity for the middle of the channel.

It should be noted that a statistical comparison (ANOV) between

Table 1

CURRENT GROSS INFORMATION

Gross	Size (cm)	Width/Depth	Drag Area (cm^2)	Submerged Mass (g)
A1	40x80	2.0	3200	2800
A2	40x80	2.0	3200	1800
A3	40x80	2.0	3200	1200
B1	25x50	2.0	1250	2200
B2	25x50	2.0	1250	1200
B3	25x50	2.0	1250	600
C1	12x30	2.5	360	2000
C2	12x30	2.5	360	1000
C3	12x30	2.5	360	400

the current crosses and the Marine Advisers ducted B-10 bi-directional, five-blade impeller meter permanently installed at station 13 yielded mean velocities significantly different (.95 level) by 5.5%. The ducted meter gave the lower velocities. The discrepancy was attributed to marine growth in the duct.

C. Salinity Measurements

Conductivity and temperature were also measured at one meter intervals from the surface to the bottom whenever velocity readings were made. A Martek water quality monitoring system, Mark I series, with a company specification of ± 0.2 mmhos cm^{-1} and ± 0.1°C respectively, was used. Using tables prepared at the Chesapeake Bay Institute of the Johns Hopkins University (unpublished manuscript), the salinity was calculated from the conductivity and temperature measurements. Temperatures and salinities are tabulated in the appendix.

The temperature fluctuations were largely of the diurnal kind. Still, the variations were minute, and the salinity distribution is therefore for the present purpose an adequate indicator of the density distribution. The temperature measurements will not be considered further.

D. Wind Measurements

Wind speed and direction were measured every 15 minutes at station 13, five meters above the mean water surface, using a Climet Model CI-9C Digital Wind System. The records are shown in Figure 5.

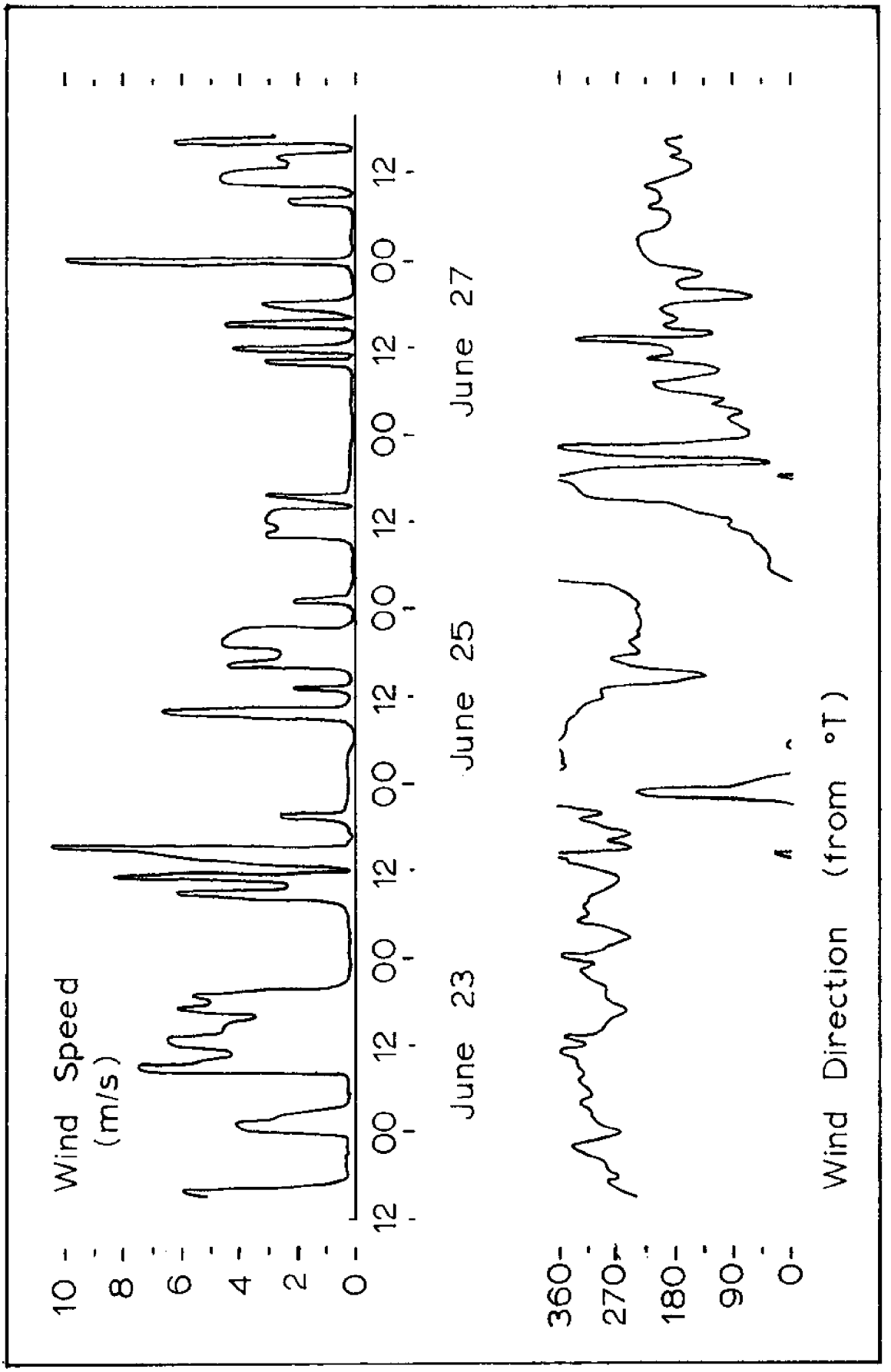

Figure 5. Wind speed and direction records as measured at station 13. The time is CDT.

For 75% of the study period, the wind blew with a westerly component: from 270-360°T 45% of the time, and from 180-270°T 30% of the time. Accordingly, the wind only contained an easterly component 25% of the time. More important, considering only winds with velocities exceeding 5 m s^{-1} (arbitrary choice): 79% of these blew from 270-360°T, and 19% from 180-270°T. Only 3% of the winds faster than 5 m s^{-1} contained an easterly component.

ANALYSIS AND DISCUSSION

A. Velocity Distribution

The instantaneous velocity distribution in the study area during each of the six tidal stages is presented in Figures 6a-f. The figures show the depth-averaged velocity, $\overline{V(t)}$, for the middle of the channel, where

$$\overline{V(t)} = \frac{1}{d(t)} \int_0^{d(t)} V(z,t)\, dz \; ; \qquad (3)$$

where d(t) is the time-dependent mid-channel depth, 0 represents the free surface (i.e., z-axis is positive down), and V(z,t) is the time- and depth-dependent velocity half-way between the banks. The integration of equation 3 was performed by planimeter. For details of the vertical velocity structure, the reader is referred to the appendix.

As the tide ebbs, the water in the tri-lake area converges at station 6, flows east into Bay Macoin, and continues east into Caminada Bay via Leon's Cut (station 3) and Bayou St. Honore (station 5). During flood tide the picture is reversed: water enters Bay Macoin via stations 3 and 5 and is forced into the tri-lake system via station 6.

It is of interest to notice that ebbing tide on the average lasted for four stages, 1-4, while flooding conditions only prevailed during stages 5 and 6. This agrees with the earlier observation that the tidal rise on the average lasted 25 minutes longer than the falling tide. This tidal asymmetry can probably largely be explained in terms of a combination of fresh water run-off and the predominantly westerly winds during the field investigation period. However, it does not

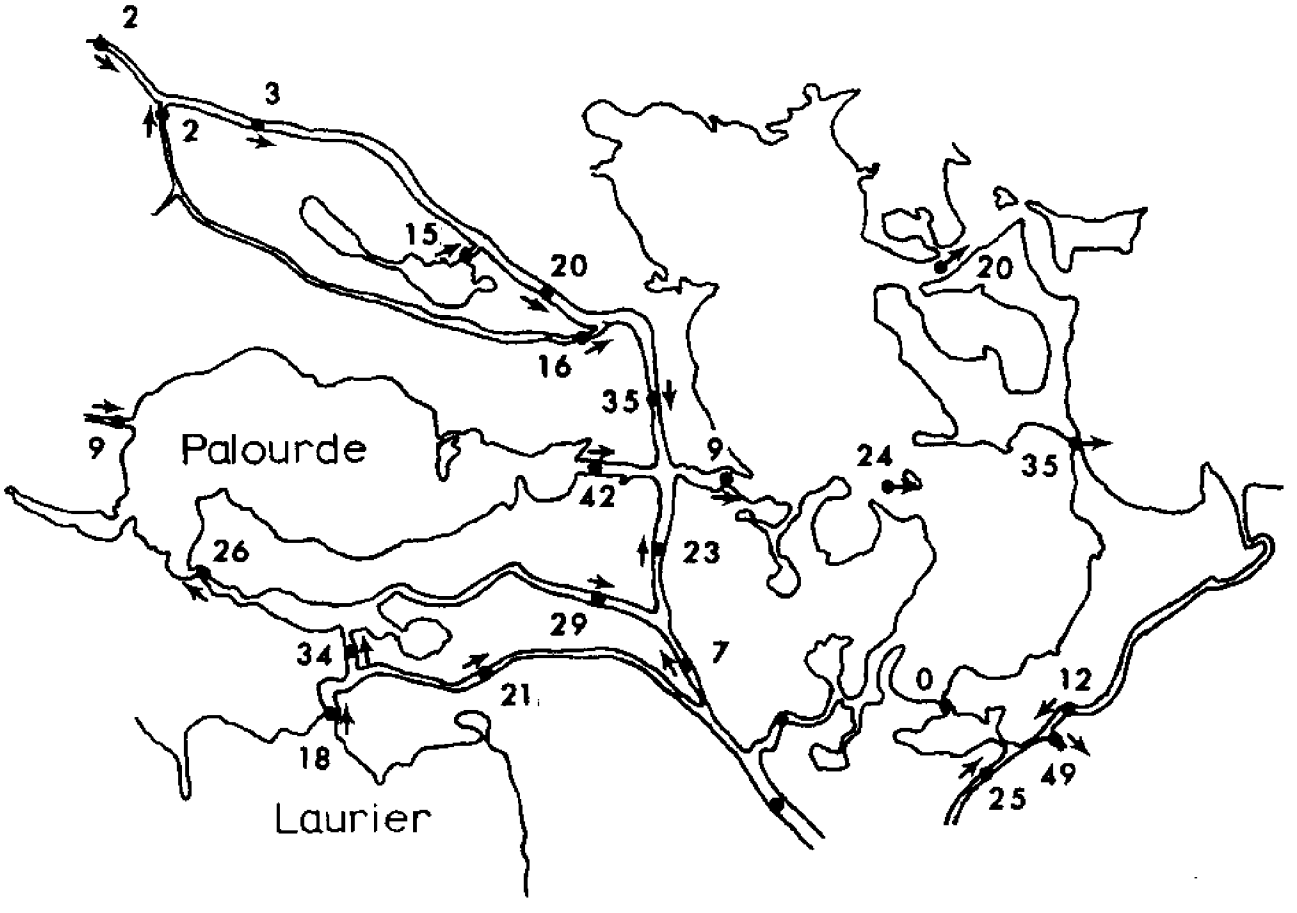

Figure 6. Depth-averaged mid-channel velocities (cm/s) and directions for the six tidal stages. a. Stage 1.

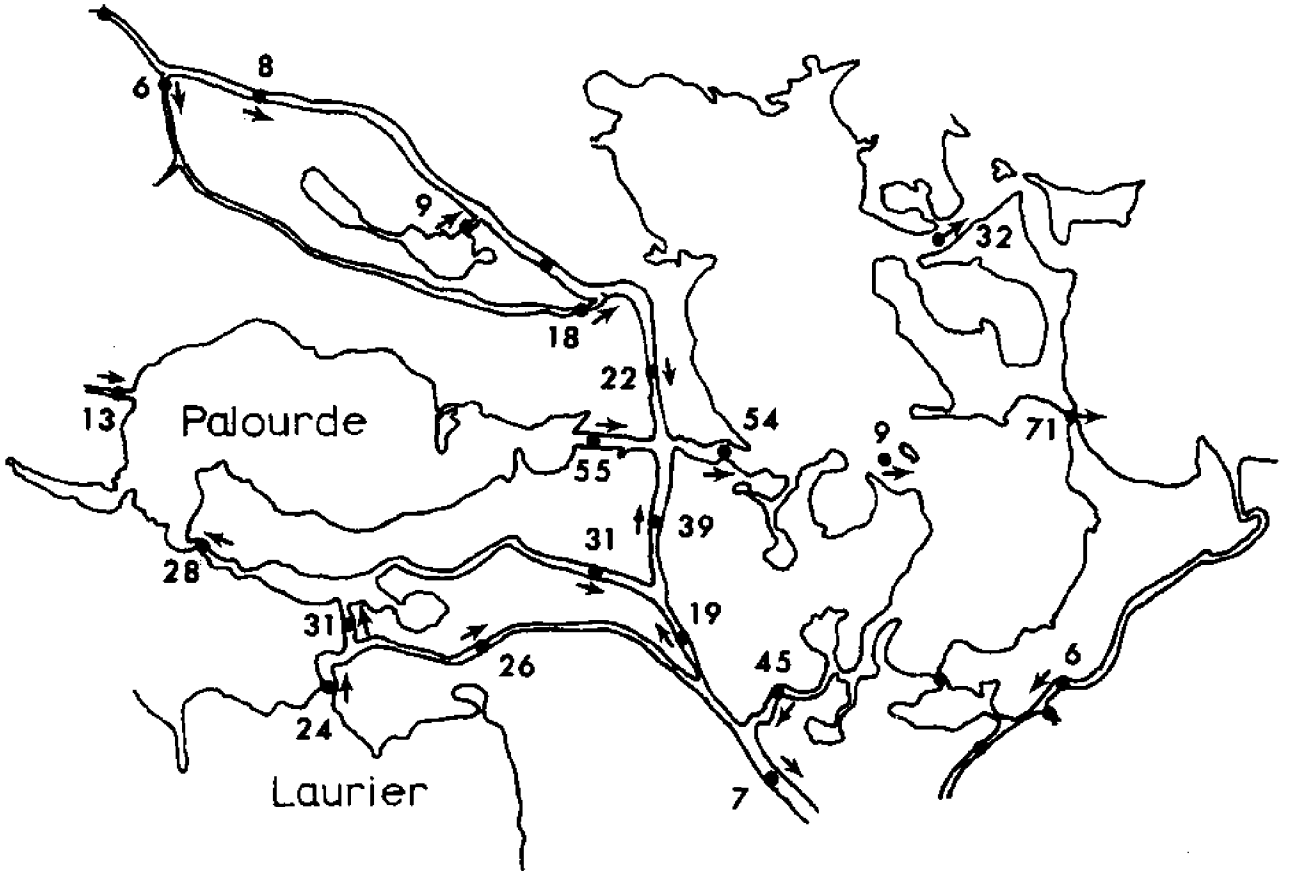

Stage 2

Figure 6b. Stage 2.

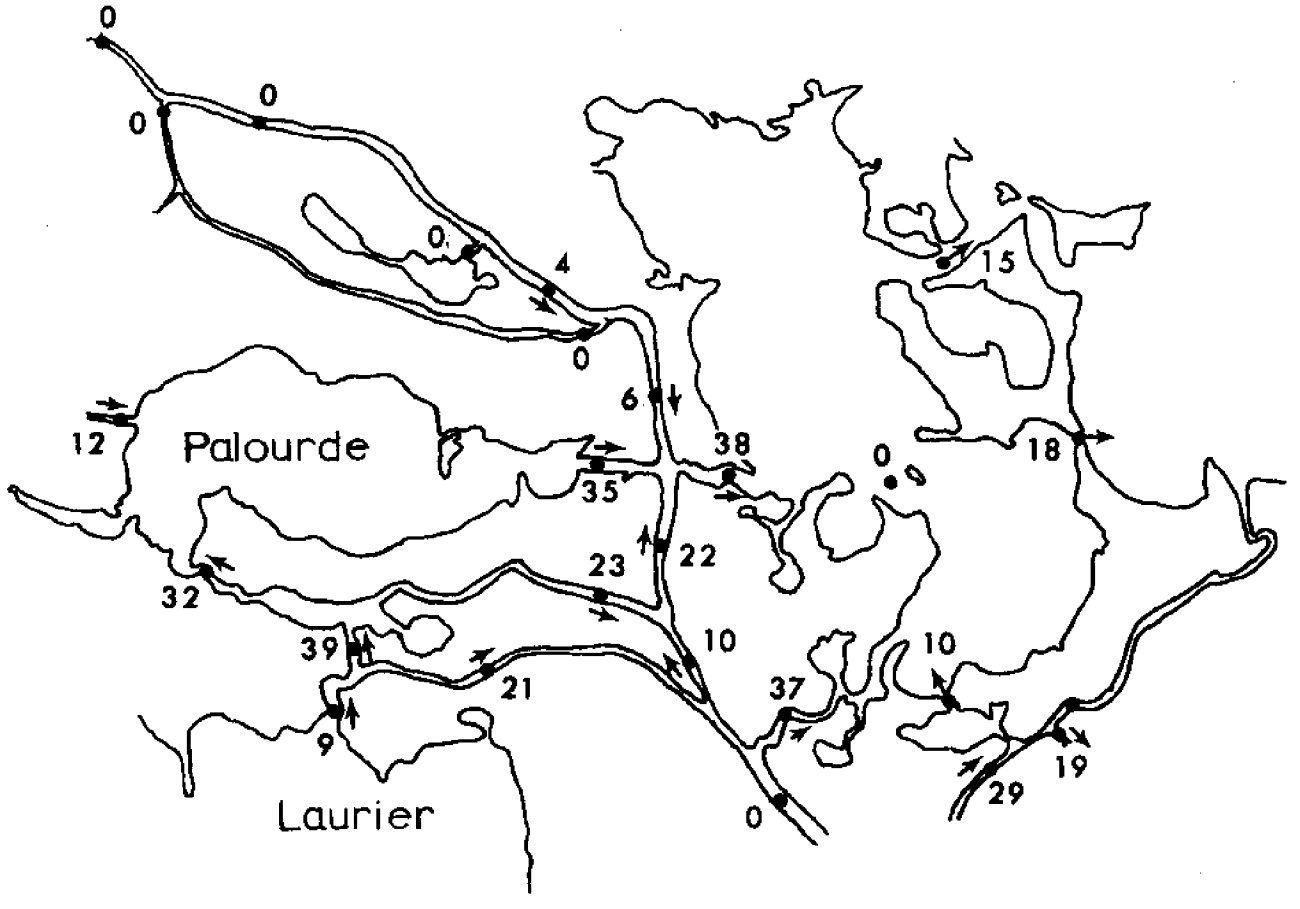

Figure 6c. Stage 3.

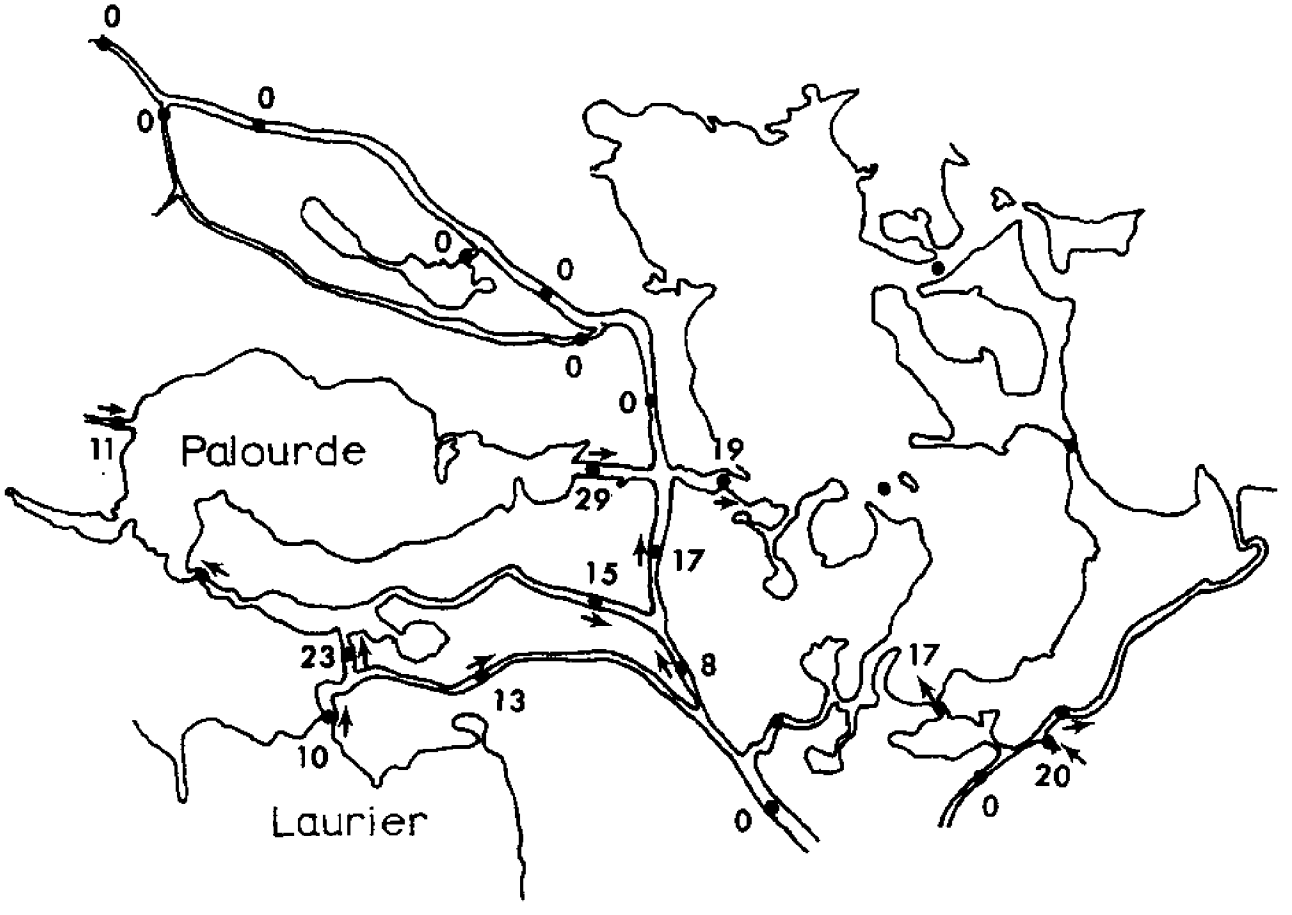

Figure 6d. Stage 4.

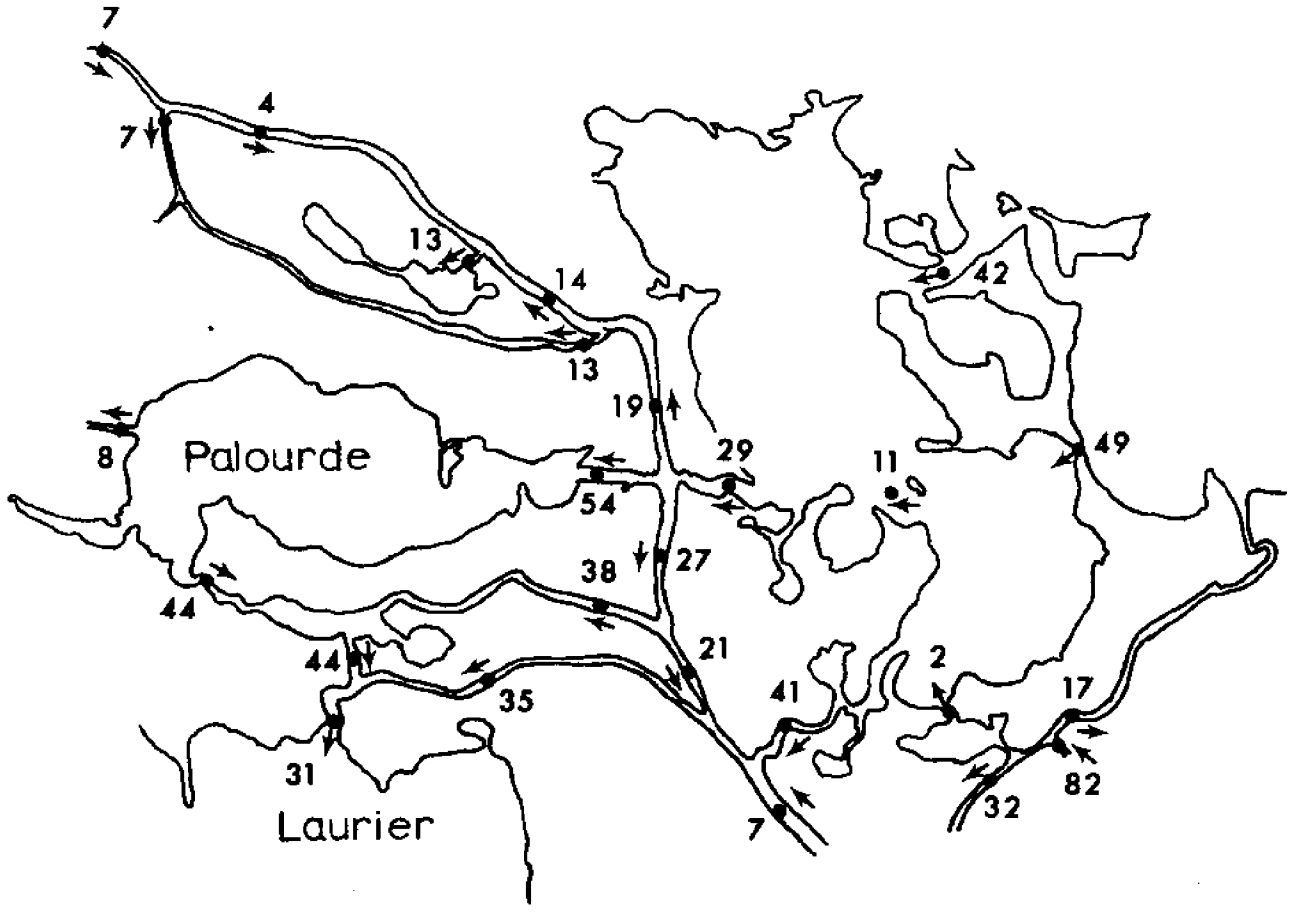

Stage 5

Figure 6e. Stage 5.

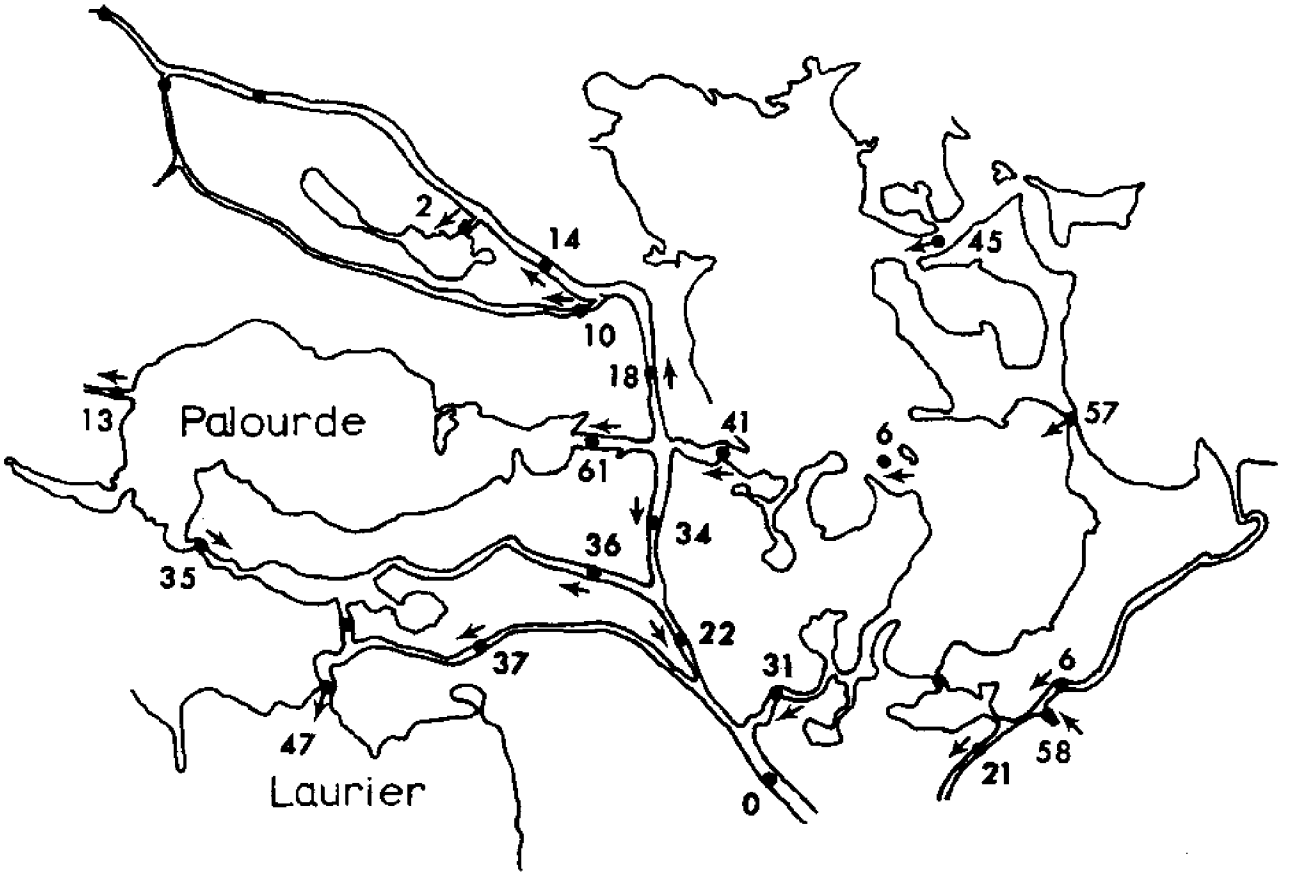

Figure 6f. Stage 6.

explain the reason that flood velocities were somewhat greater than the corresponding currents during ebb tide. Also, the indicated flow directions were in remarkable agreement during each stage.

The three lakes serve in somewhat different capacities. Lake Palourde functions as a wide channel through which water is transported to and from Lake Laurier. Lake Laurier and Airplane Lake on a smaller scale are dead end systems where water accumulates during rising tides and is removed during falling tides. This could possibly have a number of biological and geological implications.

B. Net Volume Flow

The net or time-averaged flow is probably the most desirable quantity for a multitude of purposes. However, it is usually not easy to determine as the velocity distribution in a natural channel cross-section varies irregularly, changes with time, and therefore requires considerable effort to calculate. Below is a proposed scheme to estimate the net flow from the observed data.

The velocity at any station and time varied unpredictably in the vertical. However, the lateral variation at any depth appeared to have the shape of a parabola with vanishing velocities at the banks. This was noticed at several stations and also agrees with measurements by Hacker (1972). The lateral velocity distribution just below the surface at station 2 during tide stage 1 is shown in Figure 7.

Deviation from this pattern was only observed at station 18 during stages 5 and 6 (Fig. 7), when a laterally bi-directional flow existed. Although such a flow pattern could have occurred unnoticed at

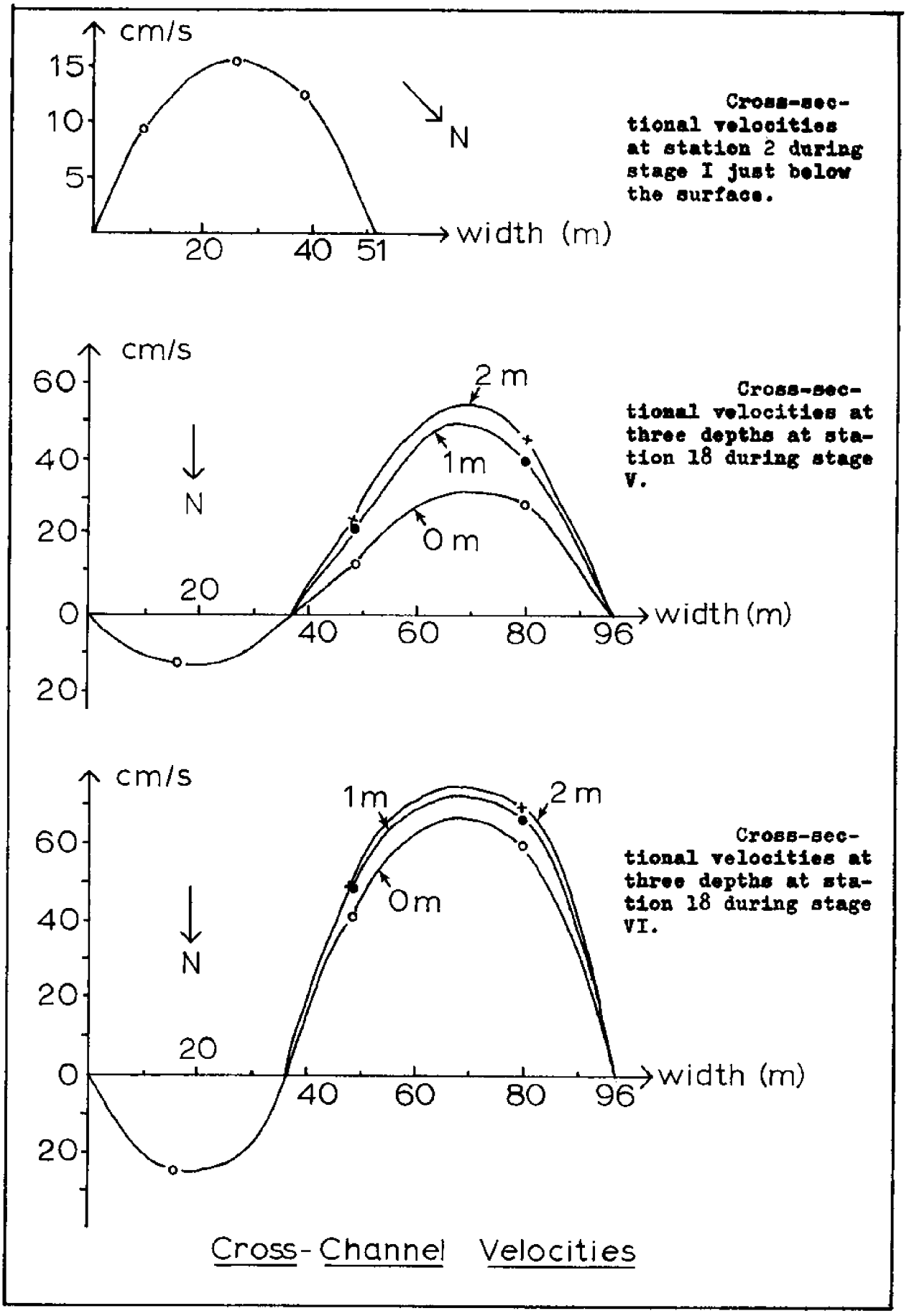

Figure 7. Cross-channel velocities.

other locations, it is assumed that this was not the case; rather that the flow at all times and stations (excluding numbers 18 and 4, which were located in open water) was unidirectional with a parabolic lateral profile at all depths. If the cross-section at each station is taken to be triangular (compare Figure 3) with the velocity measurements taken above the deepest point, it is possible to derive (see appendix),

$$Q(t) = \frac{4B_o}{3}\left[\int_0^{d(t)} V(z,t)\,dz - \frac{1}{d(t)}\int_0^{d(t)} zV(z,t)\,dz\right]; \quad (4)$$

where Q(t) is the instantaneous volume flow at a station, B_o is half the surface width, d(t) is the mid-channel depth, and V(z,t) is the measured velocity as a function of depth and time. The resulting values for the discharge, Q(t), have been tabulated in Table 2. The net volume flow at each station was finally obtained by planimetering discharge versus time plots, using a mean tide period of 24.25 hours. The resulting net volume distribution is shown in Figure 8. It is surprising to see how well flow continuity seems to be satisfied throughout the system in spite of the many assumptions which had to be made.

In general, there was a time-averaged flow passing through the study area. Water entered the tri-lake site through the cross-sections at stations 12 and 15 (note that station 18 is believed to be the only significant channel into Lake Laurier) and left primarily through the section at station 6. It is apparent that more water left than entered the system during the study period; on the average 6.9 $m^3\ s^{-1}$, considering inflow at stations 12 and 15 and outflow at stations 6 and 24. This

Table 2

TOTAL CROSS-SECTIONAL FLOW, Q, AS A FUNCTION OF TIME IN $M^3 S^{-1}$

Discharge and Flow Direction

Station	Stage I	Stage II	Stage III	Stage IV	Stage V	Stage VI	Surface Width $2B_o$ (m)
1	8.5 SE	?	3.0 SE	3.0 NW	12.1 NW	9.9 NW	16.5
2	1.1 W	0.5 W	?	0.4 E	1.4 E	0.5 W	52
3	34.7 E	69.6 E	19.4 E	?	51.9 SW	59.8 SW	41
4	-	-	-	-	-	-	-
5	40.6 E	62.8 E	30.0 E	?	90.8 W	90.8 W	145
6	14.7 E	66.7 E	48.8 E	20.3 E	35.8 W	57.7 W	122
7	8.2 S	4.0 S	0.7 S	0.0 -	3.7 N	4.0 N	50
8	1.1 E	1.0 E	0.0 -	0.0 -	0.6 W	0.7 W	20
9	5.2 SE	?	1.0 SE	0.0 -	2.8 NW	3.3 NW	70
10	0.7 SE	1.3 SE	0.0 -	0.0 -	0.5 SE	?	65
11	0.1 N	0.2 S	0.0 -	0.0 -	0.2 S	?	15
12	0.8 SE	?	0.0 -	0.0 -	1.2 SE	?	60
13	2.3 NE	1.0 NE	0.0 -	0.0 -	1.5 SW	0.3 SW	38
14	23.4 E	31.3 E	17.3 E	16.4 E	31.3 W	37.1 W	70
15	2.4 E	2.7 E	2.4 E	1.9 E	1.9 W	3.5 W	40
16	10.3 NW	10.3 NW	9.7 NW	6.4 NW	15.7 SE	14.0 SE	50
17	12.3 N	10.2 N	11.4 N	6.6 N	15.0 S	?	45
18	24.9 N	38.4 N	16.0 N	12.8 N	35.6 S*	44.0 S*	96
19	5.7 NE	6.0 NE	4.5 NE	2.4 NE	8.7 SW	10.5 SW	45
20	1.1 N	2.7 N	1.1 N	1.1 N	2.7 S	3.5 S	40
21	12.0 SE	12.0 SE	7.9 SE	4.7 SE	14.3 NW	16.0 NW	50
22	4.1 N	15.4 N	8.1 N	6.6 N	11.8 S	17.3 S	55
23	?	1.5 SE	0.0 -	0.0 -	1.5 NW	0.0 -	75
24	?	12.8 NE	10.2 NE	?	11.5 SW	10.2 SW	40
25	0.0 -	?	0.7 N	1.0 N	?	0.2 N	15
26	7.4 NE	?	5.5 NE	0.0 -	7.0 SW	5.9 SW	55

*These two values are adjusted, due to the flow behavior during ebb tide (see Fig. 7). I approximated $2B_o$=60 m rather than $2B_o$=96m as during flood tide and neglected the relatively small return (north) flow along the eastern bank.

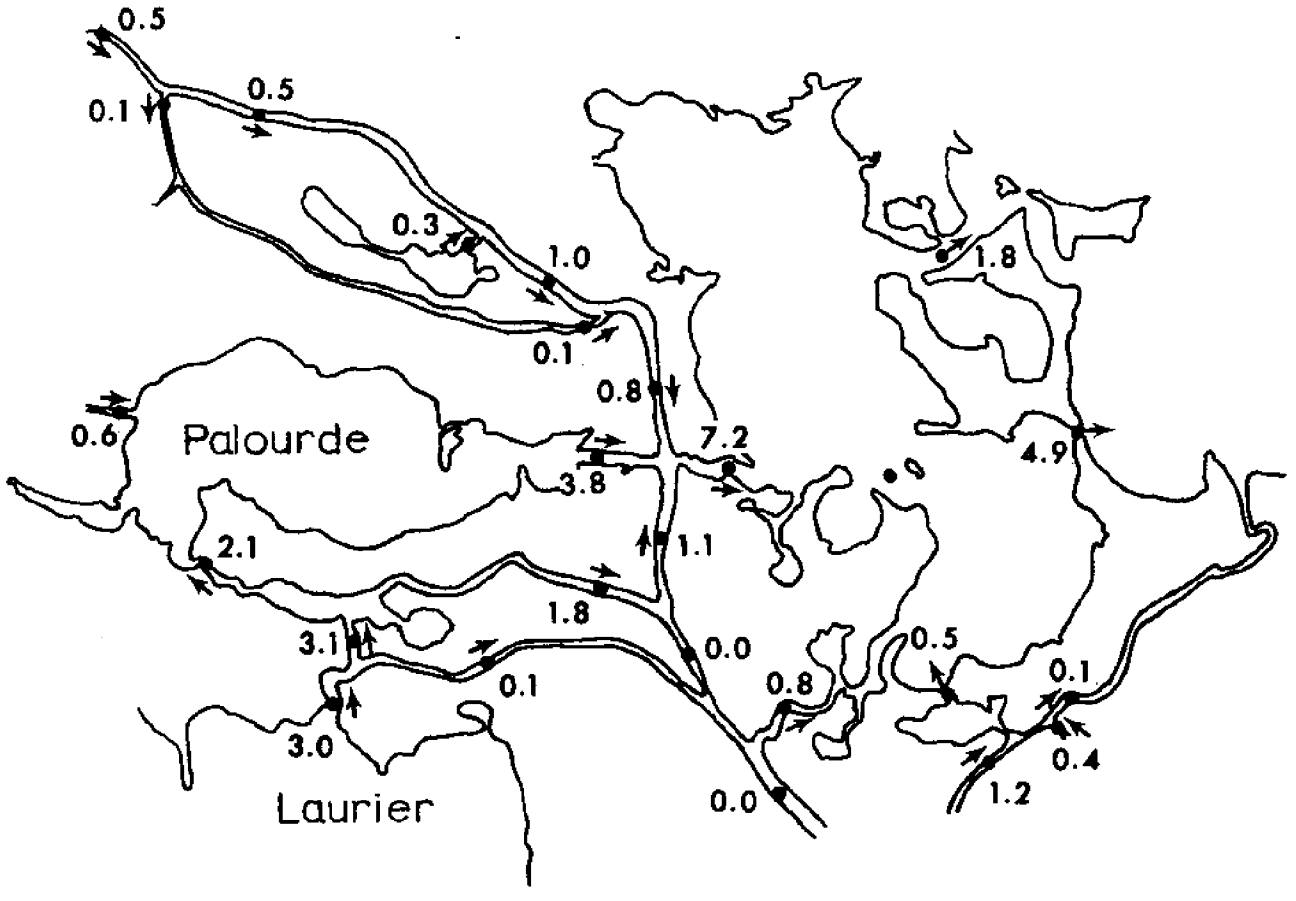

Figure 8. Net volume flow.

eastward net flow through stations 6 and 24 continued east via the cross-sections at stations 3 and 5.

Qualitatively, it is reasonable to expect winds with westerly components to move water out of the tri-lake system. Considering the wind records (Fig. 5) and the fact that the surface shear stress is approximately proportional to the square of the wind velocity, it is intuitively clear that there existed a net wind stress from the west, working to remove water from the study area during the eight-day period. Although the calculated net discharge values are only rough estimates, the overall net flow pattern appears reasonable and agrees qualitatively with the observed net shear stress due to winds with westerly components.

This is further supported by several other indications that the water level was unusually low for this time of year. Normally, a summer high pressure system in the vicinity of Bermuda drives southeasterly winds over coastal Louisiana (Leipper, 1954), which would tend to pile up water against the coast and cause relatively high water stands in the estuaries. However, during this study, northwesterly winds dominated, the water level was low, and water was being removed from the study area.

C. Net Salinity Distribution

The computed salinities have been included in the appendix. Vertical salinity gradients were usually small (less than 0.1 $^{\circ}/_{oo}$ m^{-1}) but occasionally reached much higher (greater than 1.0 $^{\circ}/_{oo}$ m^{-1}) at the stations bordering on Caminada Bay. In spite of a considerable number

of comparisons, lateral gradients were not observed at any station.

The net salinity distribution in the area was determined from the depth-averaged salinity, $\overline{S(t)}$, at each station,

$$\overline{S(t)} = \frac{1}{d(t)} \int_0^{d(t)} S(t)\, dz \quad ; \tag{5}$$

by using a planimeter. The time-averaged, depth-averaged salinity, $< \overline{S(t)} >$, for each station was then calculated from

$$< \overline{S(t)} > = \frac{1}{T} \int_0^{T} \overline{S(t)}\, dt \quad ; \tag{6}$$

where T = 24.25 hours, the mean diurnal tide period. The resulting net salinities are presented in Figure 9, with isohalines superimposed. It is apparent from the figure that fresh water primarily entered the tri-lake system from the north through Bayou Ferblanc.

D. Fresh Water Run-Off

In this case, it is impossible to assess the amount of fresh water run-off into the region from the available data without an *à priori* or independently measured knowledge of the turbulent horizontal diffusion coefficient, K_H $[L^2\ T^{-1}]$. This will become clear below.

The fresh water fraction, F, at any location in the estuary has been defined (Ketchum, 1950),

$$F = \frac{< \overline{S} >_o - < \overline{S} >}{< \overline{S} >_o} \quad ; \tag{7}$$

where $< \overline{S} >_o$ is the time- and depth-averaged reference salinity at the entrance to the system, taken to be station 6. $< \overline{S} >$ is the same

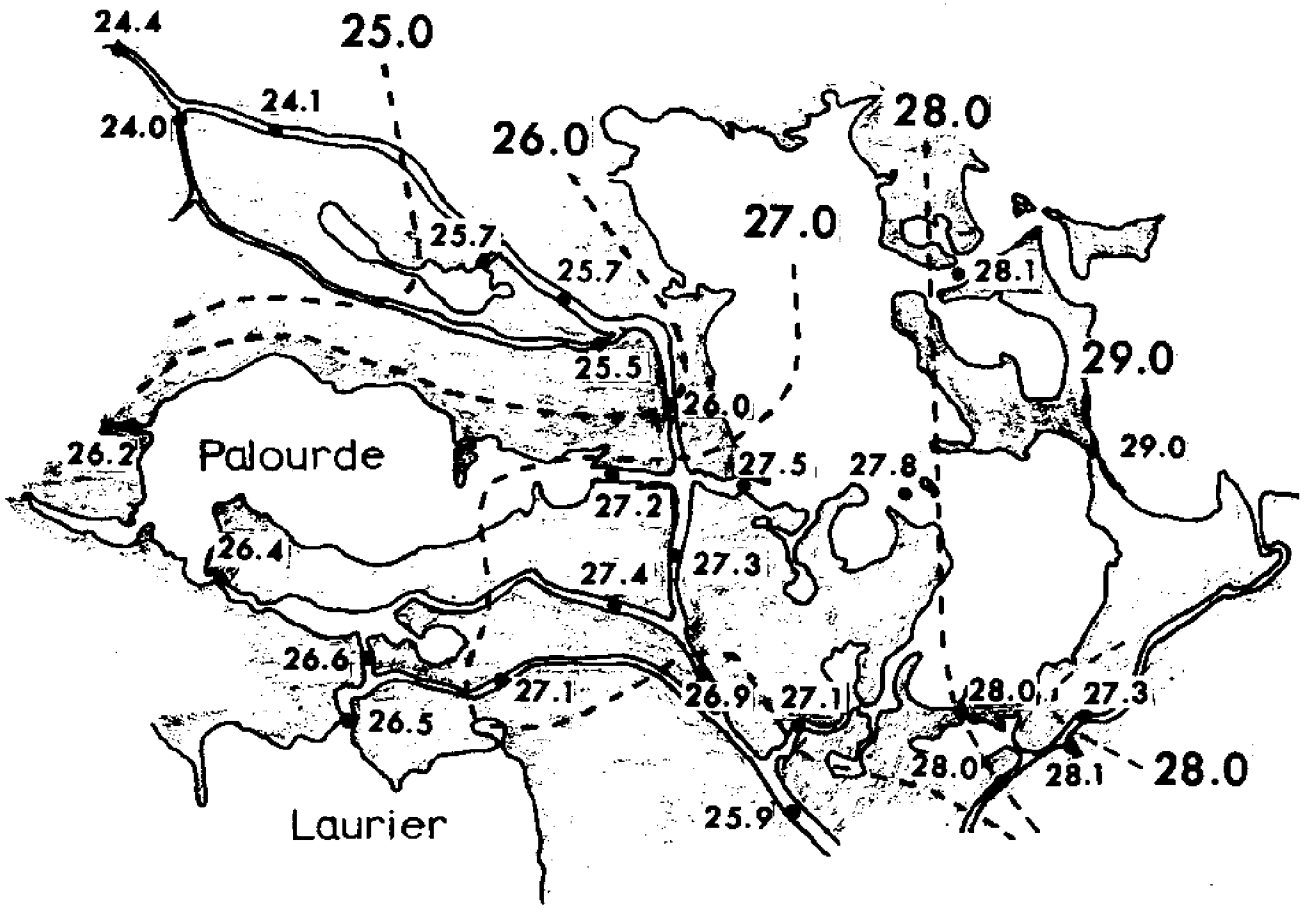

Figure 9. Time and depth salinities.

quantity at arbitrary locations within the area; here stations 12 and 15 are considered.

Equation 7 neglects diffusion processes and is therefore only an indication of the minimum fresh water run-off, as the salinity gradients are opposed to the net currents, causing a salt flux against the flow. Although Arthur (1964) presented valid continuity arguments in a hypothetical consideration of a fluid mixture with "tagged" components, for practical purposes, "fresh water" and "salt water" are not conserved. Only the total mass of the salt and the water are conservative properties (Pritchard, 1957). Therefore, equation 7 only provides information about the smallest volume (mass) of water, which entered the area as river run-off or rainfall prior to reaching stations 12 and 15. Finally, if the flow is assumed steady from tide to tide, F rather becomes the lower limit of the fraction of fresh water discharge.

The data shows that at least 11% of the flow through station 12, and at least 5% of the flow through station 15, entered the system from fresh water sources. This corresponds to very low discharges: 0.1 and 0.07 $m^3 s^{-1}$ respectively. The upper limit of F cannot be determined from the available data. It depends on the diffusion coefficient(s) and to what extent salt water had already entered Bayou Ferblanc and William Canal through connnection with some salt water source before reaching stations 12 and 15 respectively.

E. Effective Diffusion

Stommel (1953) expressed the salt balance for a vertically mixed

estuary as the balance between advective and diffusive fluxes,

$$S_{flux} = Q \; \langle \bar{S} \rangle \; - A \, K_H \, \frac{\partial \langle \bar{S} \rangle}{\partial x} \quad ; \qquad (8)$$

where S_{flux} is the net salt flux through a cross-section, Q is the cross-sectional discharge, and A is the cross-sectional area. Bowden (1963) removed the requirement of vertical homogeniety, providing that K_H was taken to be an effective horizontal turbulent diffusion coefficient.

Assuming steady conditions, $S_{flux} = 0$. Magnitudes of K_H could then be estimated from the data. Over the study period, $K_H \approx 7 \times 10^2$ $m^2 \; s^{-1}$ in Bayou Ferblanc (between stations 6 and 12) and $K_H \approx 14 \times 10^2$ $m^2 \; s^{-1}$ in Lake Palourde (between stations 6 and 15) where wind induced mixing probably caused the greater effective diffusion coefficient. In comparison, these values are one order of magnitude greater than the coefficients calculated by Bowden (1963).

The calculated coefficients for the tri-lake system are upper limits rather than actual magnitudes, as it was not possible to account for the amount of salt water advected into the area together with the fresh water run-off. These calculated upper limits of effective horizontal diffusion coefficients cannot be used to estimate the actual fresh water discharge into the system.

F. Renewal Time

Pritchard (1960) estimated the intertidal volume of Chincoteague Bay to be 11.3% of the total bay volume at mean tide. Considering the

area bounded by stations 6, 12, 15, 23, and 24 (approx. 10 km^2 of surface water area; an estimated mean volume of 1.2×10^7 m^3), the corresponding percentage for the tri-lake system was considerably greater, approximately 25%.

The renewal time or time required to replace a chosen percentage of the water in an estuary was calculated by Pritchard (1960). He let

$$\frac{dC}{C} = -\gamma \, dt \quad ; \tag{9}$$

where C is the number of "water parcels" present in the area at an arbitrary time t, dC is the number of water parcels leaving the area in the time interval dt, and γ is the percentage of these parcels flushed out from the system during each mean tidal cycle. Integration of equation 9 yields

$$\ln (C / C_o) = -\gamma (t - t_o) \quad ; \tag{10}$$

where C_o is the number of parcels present at an arbitrary starting time, t_o. The required time to replace 50% of the water present at t_o, the 50% renewal time, $t_{0.50}$, can be calculated from equation 10, setting $(C / C_o) = 0.5$. Then

$$t_{0.50} = 0.693 / \gamma \quad ; \tag{11}$$

Similarly, the 99% renewal time, $t_{0.99}$, is given by

$$t_{0.99} = 4.605 / \gamma \quad ; \tag{12}$$

Again, consider the area bounded by stations 6, 12, 15, 23, and 24. It then seems reasonable to assume that most of the water which enters the system during a flood tide is a portion of the water which

left the system during the previous ebb tide. The enclosure provided by Bay Macoin and Bay Ronfleur supports this assumption. From Pritchard (1960), it then follows that γ is the net area discharge ($8.0\ m^3\ s^{-1}$) divided by the mean system volume ($1.2 \times 10^7\ m^3$), or $\gamma = 0.058$ per mean diurnal tidal cycle. The 50% and 99% renewal times are calculated to be 12 and 80 diurnal cycles respectively, somewhat longer than the corresponding renewal times for Chincoteague Bay.

Note that the calculated renewal times are still relatively short because of the large, wind-induced, net outflow. Normal conditions for June is believed to correspond to zero net wind stress from the west, and would probably yield a net discharge similar to the net inflow at stations 12 and 15. If such were the case, the renewal times would rather be 96 and 640 diurnal cycles respectively. However, this has little meaning as steady state conditions certainly do not prevail either for 22 or for 3 months.

To obtain better estimates of renewal times, γ must be determined more accurately. This can be done, using the procedure outlined by Pritchard (1960). It requires a knowledge of the area mean salinity, the fresh water run-off, and the salinity at the mouth of the system (e.g., station 6) over a longer period.

SUMMARY

This study provides a description of some aspects of the physical oceanography of a small portion of Louisiana's estuaries, based on field measurements during an eight-day period in June, 1971.

The prevailing wind was and probably is the major factor in controlling the net water cirulation. However, the net volume flow is only a fraction of the instantaneous tidal currents. The tidal velocities were commonly on the order of 10 cm s^{-1} with a maximum observed value of 95 cm s^{-1} 1 meter below the surface during state V at station 1. The tidal currents provide energy for turbulent mixing, which resulted in nearly uniform salinities in the lateral and vertical.

Fresh water enters the system mainly from the northwest through Bayou Ferblanc. It was not possible to determine the rate of fresh water inflow from the data, only a minimum discharge value. Indications are that at least 11% of the net flow at station 12 was from rainfall or river run-off.

The effective horizontal eddy diffusivity was calculated to be not greater than approximately 10^3 m^2 s^{-1}, a quite high value, possibly indicating the importance of the wind as well as the tide in inducing mixing.

The 50% water renewal time was calculated to be 12 diurnal tidal cycles. The 99% renewal time was found to be 80 cycles, although the design of the sampling program treated the system as being in steady state, which makes the 99% renewal time meaningless in practice.

In terms of the Sea Grant program at Louisiana State University as a whole, this study indicates some of the physical oceanography

conditions other investigators can expect to encounter in the field and may want to base their sampling designs on. The next logical step would be to undertake a detailed field study of some representative area, e.g. Lake Palourde versus Lake Laurier, in terms of circulation patterns, salinity distribution, flushing, and the changes of these conditions and changes in biological, geological, and chemical parameters, and later used for prediction. As an example of this, Walls (1972) demonstrated that the activity of snapping shrimp (genus Alpheus) was far greater in locations of high net currents (stations 6 and 14) as compared to Bayou Ferblanc (stations 12, 10, 9, 7, 22, and 23) with low net discharge.

REFERENCES

Adams, R. D. 1970. A data acquisition system for measurement of meteorologic-hydrologic parameters in a remote estuarine environment. Louisiana State Univ., Coastal Studies Bull. 5:9-23.

Arthur, R. S. 1964. The equations of continuity for sea water and river water in estuaries. J. Mar. Res. 22:197-202.

Bowden, K. F. 1963. The mixing processing in a tidal estuary. J. Air and Water Poll. 7:343-356.

Foerster, J. W. 1968. A portable non-electric current meter. Chesapeake Science 9:52-55.

Hacker, S., C. W. Billups, B. Wilkins, Jr., and R. W. Pike. 1970. Hydrologic and shrimp population models. Louisiana State Univ., Coastal Studies Bull. 5:25-40.

Hacker, S., R. W. Pike, and B. Wilkins, Jr. 1971. Analysis of the energy, mass, and momentum transfer in the Louisiana coastal marsh region. Louisiana State Univ., Coastal Studies Bull. 6:109-153.

Hacker, S. 1972. Louisiana State University. Personal communications.

Ketchum, B. H. 1950. Hydrographic factors involved in the dispersion of pollutants introduced into tidal waters. J. Boston Soc. Civ. Eng. 37:296-314.

Leipper, D. F. 1954. Marine meteorology of the Gulf of Mexico, a brief review. U.S. Fish and Wildlife Service, Fishery Bull. 55(89):89-98.

Marmer, H. A. 1947. The tide in Barataria Bay. Coast and Geodetic Survey, unpublished manuscript. 23 pp.

Pritchard, D. W. 1957. Discussion of 'On estimating streamflow into tidal estuary' by K. Todd and Leung-Ku Lau. Trans. Am. Geophys. U. 38:581-583.

Pritchard, D. W. 1960. Salt balance and exchange rate for Chincoteague Bay. Chesapeake Science 1:48-57.

Pritchard, D. W. and W. V. Burt. 1951. An inexpensive technique for obtaining current profiles in estuarine waters. J. Mar. Res. 10:180-189.

Rouse, H. 1961. Fluid Mechanics for Hydraulic Engineers. Dover, N.Y. 422 pp.

Stommel, H. 1953. Computation of pollution in a vertically mixed estuary. Sewage and Industrial Wastes 25:1065-1071.

Walls, H. E. 1972. Ambient underwater acoustical noise in the estuaries of Barataria Bay. M.S. thesis. The Department of Electrical Engineering, Louisiana State University. 37 pp.

APPENDICES

Appendix A

DERIVATION OF EQUATION 4, AN EXPRESSION FOR THE VOLUME FLOW, Q(t)

Consider a right-handed coordinate system, u positive in the flow direction, and z positive down. At any one time, let the velocity through the y-z plane be u(y,z), and let V(z) be the measured velocity in mid-channel as a function of depth. V(z) is assumed to coincide with the parabola vertex. Considering a parabolic velocity distribution laterally,

$$y^2 = -4p\,[u(y,z) - V(z)] \quad ; \tag{A 1}$$

where p is the "distance" between the parabola vertex and focus. The velocity must vanish at the boundaries, i.e.,

$$u[y = \pm\, b(z)] = 0 \quad ; \tag{A 2}$$

where the bank coordinates are $\pm\, b(z)$. This yields

$$p = \frac{b(z)^2}{4\,V(z)} \quad ; \tag{A 3}$$

and equation A 1 can be rewritten,

$$u(y,z) = -\frac{V(z)}{b(z)^2}\, y^2 + V(z) \quad ; \tag{A 4}$$

Integration of equation A 4 first with respect to y from -b(z) to b(z) and then with respect to z from 0 to the bottom, d(y), yields

$$\int_0^{d(y)} \int_{-b(z)}^{b(z)} u(y,z)\, dy\, dz = \frac{4}{3} \int_0^{d(y)} b(z)\, V(z)\, dz \quad ; \tag{A 5}$$

where the left side represents the cross-sectional discharge, Q at any one time. Approximate each cross-section by a triangle, denote the time-constant surface width at any cross-section by $2B_o$, and assume the deepest, d, point to be located in mid-channel. Then, from geometry

$$b(z) = B_o - \frac{B_o z}{d} \quad ; \qquad \text{(A 6)}$$

which substituted into equation A 5 yields

$$Q = \frac{4 B_o}{3} \left[\int_0^d V(z)\, dz - \frac{1}{d} \int_0^d z\, V(z)\, dz \right] \quad ; \qquad \text{(A 7)}$$

Equation 4 in terms of Q(t) results when the time-dependence is introduced into equation A 7, noting that d and V are time-dependent, while B_o is not.

The first integral in equation A 7 times the factor $4 B_o/3$ would be the discharge if the shape of the cross-sections had been rectangular. The second integral in equation A 7 can therefore be considered as a correction factor due to the triangular shape of the cross-section. This integral was evaluated numerically for all stations, stages, and visits. The first integral was earlier evaluated in calculating the depth-averaged velocities.

Appendix B

VELOCITY, SALINITY, AND TEMPERATURE DATA

Station	Stage	Depth (m)	Correc.* (deg.)	Vel. (cm/s)	Dir.	Sal. (°/₀₀)	Temp. (°C)
1	1	0	10	44	SE	27.9	30.0
		1		44	SE	27.8	30.1
1	1	0	20	57	SE	26.5	31.9
		1		74	SE	27.3	31.5
		2		59	SE	26.8	31.5
		3				27.3	31.3
1	3	0	15	20	SE	29.4	30.8
		1		22	SE	29.3	30.8
1	4	0	10	17	NW	29.5	29.7
		1		22	NW	31.9	26.0
		2		22	NW	31.0	27.5
		3				31.0	27.5
1	5	0	35	79	NW	27.4	30.1
		1		95	NW	27.4	30.1
1	6	0	20	61	NW	26.2	27.0
		1		66	NW		
		2		53	NW		
		3		53	NW		
2	1	0	0	16	SW		
2	2	0	0	12	SW	25.8	29.7
2	2	0	0	7	SW	27.8	29.7
2	4	0	0	11	NE	29.2	29.8

*In order to arrive at the correct depth for each of the velocity measurements, the cosine of the correction should be multiplied with the noted depth. As the measured velocity gradients were small and the depths shallow, I consider it sufficient to use an average (the surface value is excluded in the average) correction for each station and time. The salinity and temperature readings need not be depth corrected as the conductivity-temperature sensor was lowered almost vertically.

Station	Stage	Depth (m)	Correc. (deg.)	Vel. (cm/s)	Dir.	Sal. (°/₀₀)	Temp. (°C)
2	5	0	0	22	NE	28.4	30.1
2	6	0	0	0	-	27.0	25.7
2	6	0	0	17	SW	25.7	30.5
3	1	0	10	30	E	27.5	31.0
		1		36	E	27.9	30.5
		2		40	E	28.7	30.3
		3		40	E	29.0	30.0
		4		44	E	29.2	30.0
3	2	0	32	71	NE	28.0	29.2
		1		77	NE	29.1	29.3
		2		77	NE	29.1	29.2
		3		76	NE	29.2	29.2
		4		81	NE	29.3	29.2
		5				29.3	29.2
3	3	0	15	32	NE	30.6	29.0
		1		27	NE	30.5	29.1
		2		27	NE	30.4	29.3
		3		23	NE	30.4	29.3
		4		19	NE	30.6	29.3
		5		15	NE	30.7	29.3
3	3	0	5	18	NE	30.3	28.2
		1		18	NE	30.6	28.9
		2		22	NE	30.7	29.0
		3		22	NE	30.7	29.1
		4		18	NE	30.7	29.0
		5		20	NE	30.6	29.0
3	5	0	35	56	SW	28.1	30.7
		1		59	SW	30.5	30.6
		2		59	SW	31.0	30.3
3	6	0	25	53	SW	26.1	27.5
		1		73	SW	25.7	27.6
		2		62	SW	25.5	27.6
		3		67	SW	25.2	28.0
		4		67	SW	25.5	27.5
4	1	0	0	30	E	28.3	30.1
4	2	0	0	12	E	28.7	30.2

Station	Stage	Depth (m)	Correc. (deg.)	Vel. (cm/s)	Dir.	Sal. (°/₀₀)	Temp. (°C)
4	3	0	0	0	-	29.0	29.0
4	3	0	0	0	-	28.4	28.6
4	5	0	0	16	W	27.3	27.8
4	6	0	0	8	W	25.5	28.5
5	1	0	12	32	E	27.7	31.0
		1		31	E	30.6	30.2
		2		20	E	31.9	29.5
5	2	0	40	29	E	27.2	29.6
		1		33	E	27.2	29.7
		2		39	E	27.2	29.7
		3		40	E	27.3	29.8
		4		37	E		
5	3	0	40	29	E	28.5	29.1
		1		37	E	29.2	29.3
		2		39	E	29.4	29.3
		3		35	E		
5	3	0	0	0	-	28.6	28.4
		1		0	-	29.1	28.5
		2		0	-	29.6	29.0
		3		0	-	30.0	29.0
5	5	0	29	46	W	27.5	31.0
		1		51	W	27.5	31.0
		2		49	W	27.5	31.0
5	6	0	40	41	W	25.7	27.3
		1		56	W	25.6	27.5
		2		55	W	25.6	27.5
		3		52	W	25.5	27.6
		4		46	W	25.2	27.5
6	1	0	6	21	E	29.1	30.1
		1		10	E	29.1	30.0
		2		9	E	29.2	30.0
6	2	0	17	53	E	27.1	29.6
		1		58	E	27.1	29.7
		2		64	E	27.2	29.7
		3		36	E	27.4	29.8

Station	Stage	Depth (m)	Correc. (deg.)	Vel. (cm/s)	Dir.	Sal. (°/₀₀)	Temp. (°C)
6	3	0	24	53	E	27.4	29.1
		1		51	E	27.8	29.3
		2		37	E	28.0	29.1
6	4	0	6	17	E	27.8	28.9
		1		20	E	28.1	29.0
		2		23	E	28.2	29.0
6	5	0	13	28	W	26.6	28.5
		1		29	W	26.9	28.2
		2		36	W	27.0	28.1
6	6	0	34	56	W	27.2	27.4
		1		54	W	27.3	27.5
		2		40	W	27.0	27.7
		3		39	W	27.2	27.6
7	1	0	34	31	S	26.6	30.0
		1		33	S	26.6	30.0
7	1	0	0	45	S	26.6	31.5
7	2	0	9	22	S	25.1	29.5
		1		27	S	25.1	29.5
7	3	0	0	9	S	25.3	29.0
		1				25.8	29.0
7	4	0	0	0	-	25.5	28.7
		1				26.6	28.4
7	5	0	0	23	N	26.6	28.0
		1				26.6	28.0
7	6	0	15	20	N	25.8	29.3
		1		21	N	25.9	29.0
8	1	0	0	18	E	26.9	32.5
8	1	0	0	22	E	26.4	32.3
8	2	0	0	21	E	24.6	29.5

Station	Stage	Depth (m)	Correc. (deg.)	Vel. (cm/s)	Dir.	Sal. (°/₀₀)	Temp. (°C)
8	3	0	0	0	-	25.0	28.3
8	4	0	0	0	-	25.7	27.2
8	5	0	0	16	W	26.5	28.1
8	6	0	0	12	W	26.2	29.2
9	1	0 1	0	21	SE	26.9 26.7	30.0 30.0
9	1	0	0	24	SE	25.1	29.1
9	3	0	0	0	SE	25.5	28.5
9	4	0	0	0	-	25.7	27.5
9	5	0	0	18	NW	26.5	28.0
9	6	0 1	0	16	NW	26.6 26.4	28.9 28.5
10	1	0	0	0	-	25.7	30.2
10	1	0	0	7	SE	24.5	31.7
10	2	0	0	11	SE	24.4	29.0
10	3	0	0	0	-	24.3	27.4
10	4	0	0	0	-	25.1	27.4
10	5	0	0	0	-	23.2	27.5
10	5	0	0	10	SE	23.3	31.2
11	1	0	0	6	N	25.7	31.2
11	1	0	0	0	-	25.3	30.5
11	2	0	0	0	S	24.6	29.0
11	3	0	0	0	-	23.9	27.8

Station	Stage	Depth (m)	Correc. (deg.)	Vel. (cm/s)	Dir.	Sal. (°/₀₀)	Temp. (°C)
11	4	0	0	0	-	24.7	27.7
11	5	0	0	0	-	23.1	26.6
11	5	0	0	15	S	22.8	31.6
12	1	0	0	0	-	26.1	29.9
		1		0	-	26.1	30.0
12	1	0	0	8	SE	25.0	28.9
12	1	0	0	0	-	25.6	30.5
12	3	0	0	0	-	24.1	28.0
12	4	0	0	0	-	26.2	26.2
12	5	0	0	0	-	23.4	28.0
12	5	0	0	15	SE	22.7	31.8
13	1	0	11	16	NE	27.0	30.1
		1		18	NE	27.4	29.9
13	1	0	0	15	NE	26.0	31.5
13	2	0	0	10	NE	25.7	29.0
13	3	0	0	0	-	25.9	28.9
13	4	0	0	0	-	25.9	26.9
13	5	0	0	17	SW	24.8	27.0
13	5	0	0	11	SW	24.9	31.3
13	6	0	3	0	-	26.3	29.5
		0.5		5	SW		
		1				26.4	29.1
14	1	0	34	42	E	27.8	31.0
		1		43	E	27.8	30.9
		2		49	E	27.8	31.0
14	2	0	20	55	E	26.3	29.5
		1		58	E	26.3	29.5
		2		56	E	26.3	29.5

Station	Stage	Depth (m)	Correc. (deg.)	Vel. (cm/s)	Dir.	Sal. (°/₀₀)	Temp. (°C)
14	3	0	9	34	E	29.7	27.9
		1		34	E	29.4	28.3
		2		42	E	30.8	27.0
14	4	0	12	28	E	28.8	28.0
		1		35	E	28.8	28.0
		2		27	E	29.2	27.5
14	5	0	29	58	W	25.2	30.9
		1		57	W	25.1	31.0
		2		53	W	25.2	30.9
14	6	0	16	71	W	26.7	27.4
		1		56	W	26.6	27.6
		2		46	W	26.5	27.9
14	6	0	32	76	W	26.5	29.0
		1		76	W	26.6	28.9
		2		76	W	26.7	28.7
15	1	0	0	10	E	27.9	29.7
15	2	0	8	13	E	26.4	30.3
		1		15	E	26.1	30.7
15	3	0	0	13	E	25.8	29.0
		1				25.8	29.1
15	4	0	0	12	E	26.1	26.4
15	5	0	0	9	W	26.2	29.1
		1				26.3	29.0
15	5	0	10	0	-	26.1	28.5
		1		10	W	26.2	28.4
15	6	0	10	14	W	25.6	28.4
		1		13	W	25.4	28.3
16	1	0	28	30	NW	27.2	29.5
		1		31	NW	27.2	29.5
		2		27	NW	27.2	29.5
16	2	0	12	30	NW	26.7	30.8
		1		31	NW	26.7	30.8
		2				26.6	30.9

Station	Stage	Depth (m)	Correc. (deg.)	Vel. (cm/s)	Dir.	Sal. (°/₀₀)	Temp. (°C)
16	3	0	15	25	NW	25.8	29.9
		1		35	NW	25.9	30.0
		2				26.4	29.0
16	4	0	14	24	NW	27.0	28.3
		1		20	NW	26.6	29.0
		2				26.6	29.0
16	5	0	33	43	SE	26.1	27.7
		1		46	SE	26.2	27.7
		2		42	SE	26.4	27.7
16	5	0	38	48	SE	26.3	28.5
		1		49	SE	26.4	28.3
16	6	0	19	36	SE	26.5	29.1
		1		39	SE	26.6	29.0
17	1	0	39	35	N	27.1	29.5
		1		36	N	27.1	29.5
		2		35	N	27.2	29.5
17	2	0	14	33	N	26.5	30.2
		1		33	N	26.5	30.5
		2				26.4	30.7
17	3	0	19	37	N	27.1	29.7
		1		41	N	27.0	30.0
		2		37	N	27.0	30.0
17	4	0	22	20	N	27.0	29.0
		1	25	25	N	27.0	29.1
17	5	0	30	50	S	26.6	27.5
		1		43	S	26.6	27.5
17	5	0	39	47	S	26.4	28.5
		1		50	S	26.4	28.2
18	1	0	16	17	N	26.4	29.8
		1		22	N	26.4	29.8
		2		21	N	26.5	29.8
		3				26.5	29.8
18	2	0	20	25	N	26.3	30.1
		1		23	N	26.3	30.2
		2		25	N	26.3	30.6
		3		25	N	26.3	30.6

Station	Stage	Depth (m)	Correc. (deg.)	Vel. (cm/s)	Dir.	Sal. (°/₀₀)	Temp. (°C)
18	3	0	1	22	N	27.1	29.9
		1		9	N	27.1	30.0
18	4	0	5	13	N	27.0	29.0
		1		7	N	26.9	29.1
		2		15	N	26.9	29.1
		3				27.0	29.2
		4				26.4	29.3
18	5	0	6	12	N	26.3	28.4
		1		22	N	26.3	28.3
		2		23	N	26.3	28.3
18	5	0	31	45	S	26.6	27.7
		1		49	S	26.6	27.7
		2		54	S	26.6	27.8
18	6	0	27	41	S	26.8	29.0
		1		48	S	26.8	29.0
		2		48	S	26.8	29.0
		3			S	26.8	29.0
19	1	0	30	21	NE	27.3	29.7
		1		23	NE	27.3	29.8
19	2	0	12	29	NE	26.5	30.6
		1		31	NE	26.4	30.7
19	3	0	7	20	NE	27.6	26.0
		1		23	NE	27.5	29.2
19	4	0	0	16	NE	27.0	29.0
		1				27.0	29.0
19	5	0	31	46	SW	26.7	27.6
		1		43	SW	27.3	26.5
19	5	0	32	32	SW	25.3	28.1
		1		32	SW	25.3	28.2
19	6	0	0	43	SW	27.8	28.5
20	1	0	0	8	NW	27.3	31.5
20	2	0	0	22	NW	27.6	30.2
20	3	0	0	11	NW	27.7	29.0

Station	Stage	Depth (m)	Correc. (deg.)	Vel. (cm/s)	Dir.	Sal. (°/₀₀)	Temp. (°C)
20	4	0	0	9	NW	27.0	28.9
20	5	0	0	24	SE	26.7	28.1
20	6	0	0	26	SE	26.2	28.7
21	1	0	16	31	SE	27.6	30.7
		1		30	SE	27.6	30.8
21	2	0	14	35	SE	26.6	30.8
		1		33	SE	26.6	30.8
21	3	0	0	27	SE	29.4	26.0
		1				29.4	25.9
21	4	0	0	18	SE	29.2	25.1
		1				28.4	26.5
21	5	0	30	40	NW	26.7	28.2
		1		42	NW	26.7	28.1
21	6	0	30	50	NW	26.3	28.2
		1		44	NW	26.3	28.1
21	6	0	30	45	NW	27.2	29.0
		1		35	NW	27.2	29.0
22	1	0	0	18	S	25.4	30.0
		1				25.3	30.0
22	1	0	16	39	N	28.6	30.5
		1		32	N	28.6	30.7
22	2	0	35	43	N	27.9	31.0
		1		43	N	27.8	31.0
22	3	0	0	25	N	29.0	27.0
22	4	0	0	22	N	27.9	27.9
22	5	0	38	40	S	26.6	27.9
		1		35	S	26.6	27.9
22	6	0	15	50	S	26.2	28.3
		1		35	S	26.2	28.3
23	2	0	0	8	SE	26.5	30.3
23	3	0	0	0	-	30.1	27.5

Station	Stage	Depth (m)	Correc. (deg.)	Vel. (cm/s)	Dir.	Sal. (°/₀₀)	Temp. (°C)
23	4	0	0	0	-	28.9	29.0
23	5	0	0	15	NW	28.8	27.2
23	5	0	0	0	-	22.4	28.1
23	6	0	0	0	-	27.7	27.7
23	6	0	0	0	-	18.5	30.0
24	2	0	0	50	NE	27.3	30.3
24	3	0	32	41	NE	27.5	28.5
		1		46	NE	27.2	29.0
		2		43	NE		
24	3	0	13	35	NE	28.7	27.6
		1		32	NE		
24	5	0	32	36	SW	26.5	27.5
		1		44	SW	26.4	27.5
24	5	0	12	44	SW	26.3	28.1
		1		44	SW	26.3	28.0
24	6	0	32	34	SW	28.2	25.6
		1		32	SW	26.9	27.9
25	1	0	0	19	N	28.1	30.3
		1				31.6	29.9
25	1	0	0	19	S	26.2	30.0
25	3	0	0	12	N	29.9	29.0
25	4	0	0	19	N	28.1	29.0
25	5	0	12	13	N	26.0	26.5
		1		12	N	26.0	26.5
25	5	0	0	9	S	25.3	27.8
		1				27.6	27.8
26	1	0	0	29	NE	27.2	30.7

Station	Stage	Depth (m)	Correc. (deg.)	Vel. (cm/s)	Dir.	Sal. (°/₀₀)	Temp. (°C)
26	3	0	0	32	NE	30.0	30.0
26	4	0	0	0	-	28.1	29.5
26	5	0	16	32	SW	28.9	27.9
		1		36	SW	28.8	27.9
26	6	0	0	38	SW	26.6	25.6
26	6	0	0	8	SW	26.6	30.2